Local order-disorder behaviour in Cr^{3+}-doped dimethylammonium aluminium sulphate hexahydrate (DMAAS) studied by electron paramagnetic resonance

2000 J. Phys.: Condens. Matter 12 4553

(http://iopscience.iop.org/0953-8984/12/21/302)

J. Phys.: Condens. Matter **12** (2000) 4553–4566. Printed in the UK PII: S0953-8984(00)09957-4

Local order–disorder behaviour in Cr^{3+}-doped dimethylammonium aluminium sulphate hexahydrate (DMAAS) studied by electron paramagnetic resonance

G Völkel†, N Alsabbagh†, R Böttcher†, D Michel†, B Milsch†, Z Czapla‡ and J Furtak‡

† Faculty of Physics and Geosciences, University of Leipzig, Linnéstrasse 5, D-04103 Leipzig, Germany

‡ Institute of Experimental Physics, University of Wroclaw, Maxa Borna 9, PL-50204 Wroclaw, Poland

Received 29 November 1999, in final form 29 February 2000

Abstract. Electron paramagnetic resonance (EPR) investigations of the ordering behaviour in single crystals of Cr^{3+}-doped dimethylammonium aluminium sulphate hexahydrate (DMAAS) are presented at the transition from the ferroelastic to the ferroelectric phase. The measurements on chromium-doped DMAAS show that the Cr^{3+} probe substitutes at aluminium sites. Remarkable line-shape changes and line splittings are observed in the EPR experiment in contrast to the findings of former ^{27}Al nuclear magnetic resonance studies. The EPR measurements confirm the order–disorder character of the ferroelectric phase transition at 151 K on a microscopic level and give information about the local order parameter of the dimethylammonium reorientation and the relation of the dimethylammonium reorientational motion to the critical dynamics.

1. Introduction

Crystals consisting of organic and inorganic molecular constituents show very often such interesting ordering phenomena as ferroelasticity, ferroelectricity, commensurate and incommensurate phases and orientational glass behaviour due to the large number of internal degrees of freedom. DMAAS belongs to a crystal family with the further members dimethylammonium gallium sulphate hexahydrate (DMAGaS)$(CH_3)_2NH_2Ga(SO_4)_2{\cdot}6H_2O$ and dimethylammonium aluminium sulphate selenate hexahydrate (DMAASe) mixed crystals $(CH_3)_2NH_2Al(S_{1-x}Se_xO_4)_2{\cdot}6H_2O$ [1–12]. The crystal structure is built up of Al or Ga cations coordinating six water molecules hydrogen bonded to regular SO_4 tetrahedra and of $[(CH_3)_2NH_2]^+$ (DMA) cations hydrogen bonded into a three-dimensional framework.

In their high-temperature phase crystals of DMAAS and DMAGaS were found to be isomorphic in structure and ferroelastic. DMAAS exhibits an anomalously large spontaneous deformation and ranks as one of the plastic crystals. Both crystals exhibit a structural transition into a ferroelectric phase. The dimethylammonium (DMA) cations play an important role in the mechanism of the ferroelectric transitions which is regarded to be of order–disorder type. DMAAS undergoes a ferroelectric transition at $T_C = 152$ K of second order whereas DMAGaS shows two successive first-order phase transitions into a ferroelectric phase at $T_{C1} = 136$ K and into the low-temperature nonpolar phase at $T_{C2} = 118$ K. The reason for this different

0953-8984/00/214553+14$30.00

behaviour is not completely understood so far. A deeper knowledge of the molecular ordering behaviour should contribute to casting some light on this open problem.

A sharp peak of the dielectric permittivity has been observed at T_C in temperature-dependent measurements along the ferroelectric $\boldsymbol{a}$-direction [11]. There is also a strong dispersion at frequencies below 1 MHz which is due to domain wall motions. Measurements of the dielectric permittivity along the $\boldsymbol{b}$- and $\boldsymbol{c}$-directions showed additional anomalies of the real and imaginary parts in the temperature range from 115 K to 95 K as well as at 75 K [1,6,8,11]. The structural nature of these anomalies is also not understood.

The crystal structure of DMAAS is monoclinic with a space group $P2_1/a$. In a crystallographic coordinate system with the $\boldsymbol{c}$-axis chosen as the monoclinic twofold screw axis and with the $\boldsymbol{a}$- and $\boldsymbol{b}$-axes forming the monoclinic angle $\gamma = 68.13^\circ$, the unit-cell parameters are $a = 11.787$ Å, $b = 6.403$ Å and $c = 10.747$ Å [7]. In the present study, a transformed coordinate system given by the relations $\boldsymbol{a}_N = \boldsymbol{a} - \boldsymbol{b}$, $\boldsymbol{b}_N = \boldsymbol{b}$, $\boldsymbol{c}_N = \boldsymbol{c}$ with $a_N = 11.787$ Å and the monoclinic angle $\gamma = 100.4^\circ$ [7] is used. It is equivalent to the coordinate system in reference [10] where, however, the monoclinic axis is assigned as the $\boldsymbol{b}$-axis. The atomic structure of the unit cell projected on the (001) plane is shown in figure 1. The ferroelastic phase is stable up to about 390 K [2]. X-ray diffraction studies showed that at the second-order transition into the ferroelectric phase at $T_C = 152$ K the twofold screw axis disappears and thereby a spontaneous polarization appears along the crystallographic $\boldsymbol{a}$-direction. The ferroelectric order is associated with the polar DMA molecules which execute hindered rotations around their C–C direction in the ferroelastic phase and order statistically along the $\boldsymbol{a}$-direction in the ferroelectric phase. As x-ray [10] and neutron scattering experiments [13] showed, at room temperature the NH_2 group of the DMA molecule is disordered over four positions related by a centre of inversion with the occupancies 0.4 and 0.1, respectively. The occupancy of the two positions with initial occupancy 0.1 at room temperature is reported to

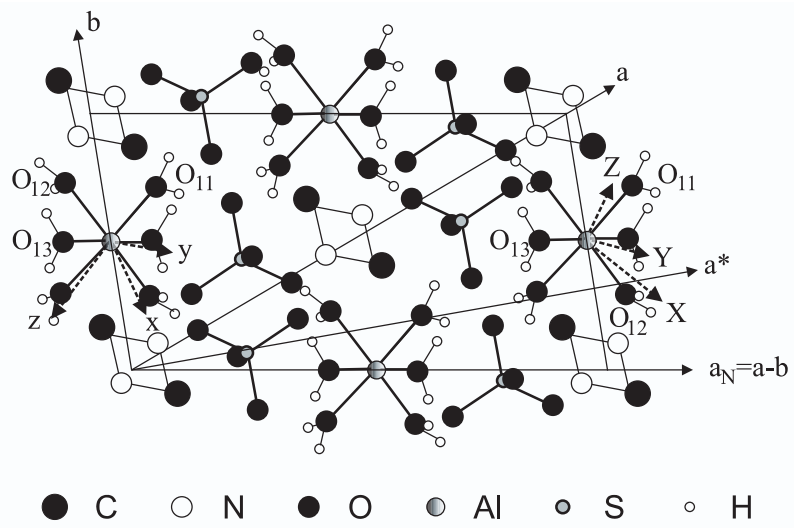

Figure 1. The crystal structure of DMAAS at room temperature. The unit cell is projected on the (001) plane of the $\boldsymbol{a}_N\boldsymbol{b}_N\boldsymbol{c}_N$-system (after [10]). The hydrogen atoms of the dimethylammonium ions as well as the two additional nitrogen positions along and opposite to the $\boldsymbol{c}$-axis are left out. The $\boldsymbol{a}^*$-axis used in the rectangular experimental coordinate system $\boldsymbol{a}^*\boldsymbol{b}\boldsymbol{c}$ and the projections of the principal axes XYZ of the Cr^{3+} fine-structure tensor and xyz of the ^{27}Al quadrupole tensor are shown by arrows.

change to 0.01 in the ferroelectric phase at 135 K [14] whereas the polar positions become fully ordered. However, a quantitative relationship of the position occupancy with the order parameter could not be derived from these data. It is now commonly supposed that below T_C the DMA molecules freeze in one position and the spontaneous dielectric polarization results in a glide mirror plane directed in parallel to the centre-of-mass DMA–DMA direction in the unit cell.

In the last year, angle-dependent ^{27}Al NMR measurements [15] on the ferroelastic and ferroelectric phases of DMAAS have been performed by some of the present authors. It has been shown that two equivalent line sets appear in the ferroelastic and ferroelectric phases as well according to the two chemically equivalent aluminium sites in the unit cell. Therefore, the ^{27}Al nuclear quadrupole tensors of the two sites are equivalent and have in a rectangular coordinate system defined by $\boldsymbol{a}^* = \boldsymbol{b} \times \boldsymbol{c}$, $\boldsymbol{b}$, $\boldsymbol{c}$ the components $Q_{a^*a^*} = -153$ kHz, $Q_{bb} = 10$ kHz, $Q_{cc} = 143$ kHz, $Q_{bc} = \pm 518$ kHz, $Q_{a^*c} = \pm 297$ kHz, $Q_{a^*b} = -655$ kHz. Diagonalization gave the principal values $Q_{xx} = 315$ kHz, $Q_{yy} = 699$ kHz, $Q_{zz} = -1014$ kHz. The principle axes form with the Al–O directions of the aluminium water octahedron the angles $\measuredangle(x, O_{12}\text{–Al–}O_{12}) = 8^\circ$, $\measuredangle(y, O_{13}\text{–Al–}O_{13}) = 6^\circ$, $\measuredangle(z, O_{11}\text{–Al–}O_{11}) = 12^\circ$. Measurements in selected directions showed temperature-dependent shifts but no splitting of the ^{27}Al quadrupolar-split satellite lines which manifest structural changes in the environment of the Al sites related to the second-order transition at $T_C = 152$ K [15]. However, it was not possible to derive more detailed information from the ^{27}Al NMR measurements about the ordering behaviour of the dimethylammonium groups.

Recently, other ^{1}H NMR and ^{27}Al NMR and NQR studies on DMAAS have been published [16] which presented a wealth of complicated temperature effects. However, the reported ^{27}Al quadrupole tensor values and the conclusion concerning inequivalent Al sites are in contrast to our former NMR and EPR [17] results. Also recent EPR measurements of other authors [18] on Cr^{3+} substituting for aluminium showed no differences between the fine-structure parameters of the two sites within the experimental errors.

The present paper deals with investigations of the reorientational order in the close vicinity of the $Cr^{3+}_{Al}(H_2O)_6$ octahedron in DMAAS by means of electron paramagnetic resonance (EPR) measurements. However, it is noted that the EPR results presented here are qualitatively different from previous magnetic resonance studies on order–disorder systems with respect to the capability to measure the order parameter quantitatively. Usually, in NMR or EPR experiments, the information about the order parameter is taken from line shifts resulting from averaging processes during the formation of the ordered state. Here, in contrast to this, the order parameter is directly obtained from the relative occupation of the disordered states involved which results from the intensity of the accompanying separable EPR lines. Due to the different timescale of the EPR spectroscopy as compared to that of NMR and the stronger spectroscopic coupling of the Cr^{3+} sites to local structural changes, the EPR method has proved to be an excellent spectroscopic technique for studying the influence of the dimethylammonium rearrangements on the static and dynamic properties of the $Al(H_2O)_6$ and the substitutional $Cr(H_2O)_6$ defect sites, respectively. It is the aim of this paper to derive more detailed conclusions on the ordering behaviour of the DMA groups by means of a direct comparison of ^{27}Al NMR and Cr^{3+} EPR measurements in the ferroelastic and ferroelectric phases.

2. Experimental procedure

Chromium-doped DMAAS single crystals were grown from aqueous solution containing 0.5 mol% $Cr_2(SO_4)_3 \cdot 18H_2O$. The trivalent chromium ions with the electron configuration

$(3d)^3$ substitute at statistically aluminium sites. Dielectric measurements show the phase transition temperature to be unchanged with doping (see figure 2). The chromium ions are paramagnetic probes imaging very sensitively the slightest changes of their environment. EPR measurements were performed at the X band (9400 MHz) and Q band (34400 MHz) using a BRUKER spectrometer of type ESP380 FT/CW with a Q-band accessory and an OXFORD CF935 cryostat. The precision of the relative temperature measurements was better than a tenth of a kelvin. The crystal coordinate system used for the angle-dependent measurements is the system $\boldsymbol{a}^*$, $\boldsymbol{b}$, $\boldsymbol{c}$ mentioned above.

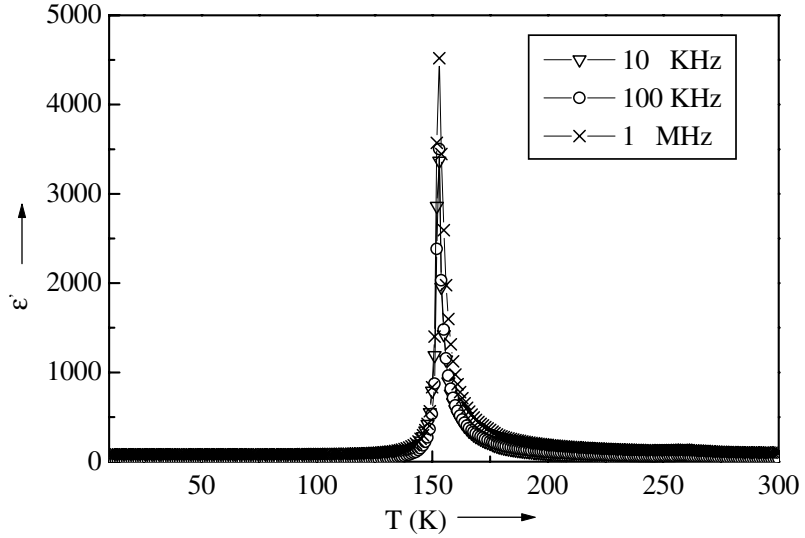

Figure 2. Temperature dependences of the real part of the dielectric susceptibility of chromium-doped DMAAS measured at frequencies 10 kHz, 100 kHz and 1 MHz along the ferroelectric $\boldsymbol{a}$-direction.

3. Results

Angle-dependent EPR measurements were performed at room temperature in three planes perpendicular to the $\boldsymbol{a}^*$-, $\boldsymbol{b}$- and $\boldsymbol{c}$-axes, respectively. The rotation patterns are shown in figure 3. Two magnetically equivalent sets of triplets are observed in accordance with the two chemically equivalent Al sites in the unit cell which can be substituted for with Cr^{3+} ions. The spectra can be described by means of the spin Hamiltonian [19]

$$\hat{H} = \beta \vec{B} \vec{\vec{g}} \vec{\hat{S}} + \vec{\hat{S}} \vec{\vec{D}} \vec{\hat{S}} \tag{1}$$

where $\vec{\hat{S}}$ is the electron spin operator of the Cr^{3+} ion with $S = 3/2$, β is the Bohr magneton, $\vec{\vec{g}}$ is the g-tensor and $\vec{\vec{D}}$ is the fine-structure tensor. A fitting procedure performed simultaneously for the Q-band results in all the three planes at room temperature leads to the following parameters: $g = 1.997 \pm 0.001$, $D_{a^*a^*} = 34 \times 10^{-4}$ cm^{-1}, $D_{bb} = -288 \times 10^{-4}$ cm^{-1}, $D_{cc} = 254 \times 10^{-4}$ cm^{-1}, $D_{bc} = 131 \times 10^{-4}$ cm^{-1}, $D_{a^*c} = 180 \times 10^{-4}$ cm^{-1}, $D_{a^*b} = -413 \times 10^{-4}$ cm^{-1}. The accuracy is $\pm 5 \times 10^{-4}$ cm^{-1}. A diagonalization gives the following principal values of the fine-structure tensor: $D_{XX} = (238 \pm 3) \times 10^{-4}$ cm^{-1}, $D_{YY} = (383 \pm 5) \times 10^{-4}$ cm^{-1}, $D_{ZZ} = (-621 \pm 10) \times 10^{-4}$ cm^{-1}, equivalent to $D = (3/2)D_{ZZ} = (932 \pm 15) \times 10^{-4}$ cm^{-1} and $E = \frac{1}{2}(D_{YY} - D_{XX}) = (73 \pm 4) \times 10^{-4}$ cm^{-1}.

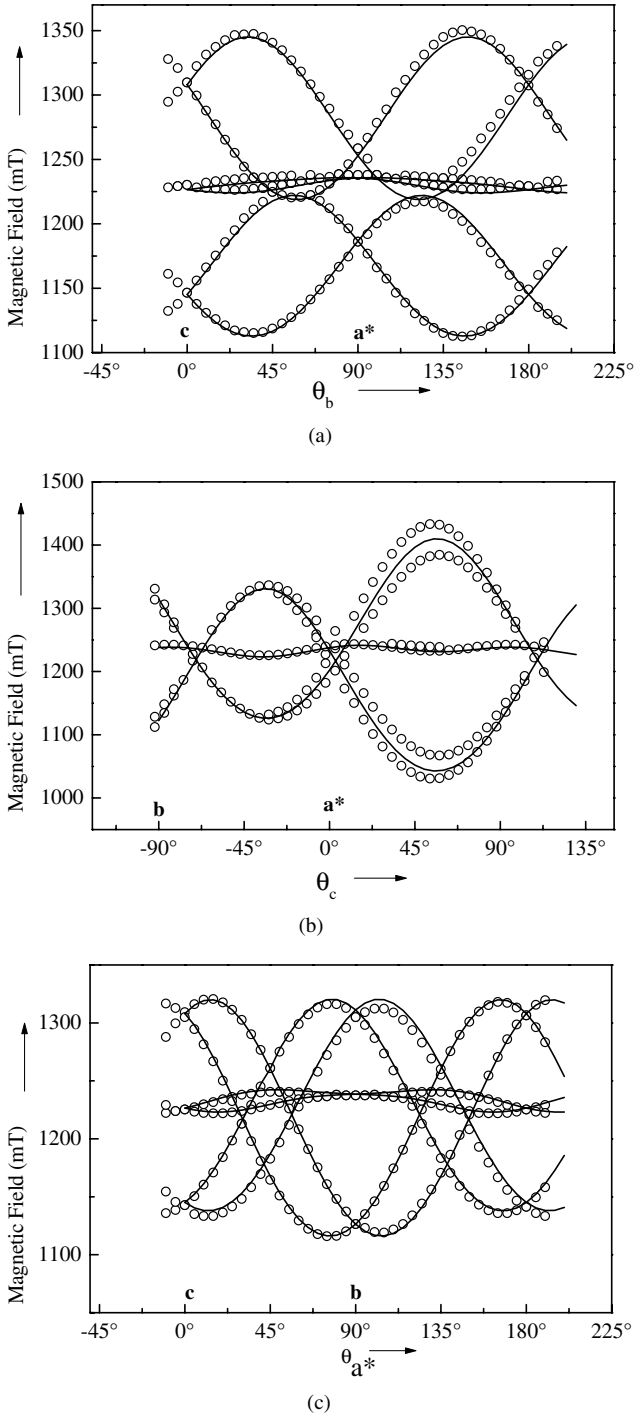

Figure 3. The angular dependence of the Cr^{3+} EPR lines in DMAAS measured at the Q band while rotating the magnetic $\boldsymbol{B}$-field in the (a) $\boldsymbol{a}^*\boldsymbol{c}$-plane, (b) $\boldsymbol{a}^*\boldsymbol{b}$-plane and (c) $\boldsymbol{b}\boldsymbol{c}$-plane of the crystal. The $\boldsymbol{a}^*$-, $\boldsymbol{b}$- and $\boldsymbol{c}$-directions are clearly seen in (a) and (c) as those orientations where the fine-structure lines of the two chromium sites collapse. The still visible line splitting in (b) is caused by a 5° misorientation of the crystal with respect to the rotation axis. The solid lines show the fit result with the parameters given in the text.

The correct simulation of the experimentally measured powder spectrum with this parameter set confirms its adequacy as seen in figure 4. The eigenvectors corresponding to the tensor principal axes with respect to the system $\boldsymbol{a}^*, \boldsymbol{b}, \boldsymbol{c}$ are obtained as $\boldsymbol{e}_X = (\pm 0.454, \pm 0.535, 0.713)$, $\boldsymbol{e}_Y = (\pm 0.690, \pm 0.296, 0.661)$ and $\boldsymbol{e}_Z = (\pm 0.564, \pm 0.792, -0.235)$. If one compares these directions with the Al–O directions in the crystal, the principal tensor axes form the following angles with the Al–O bond directions of the undistorted $Al(H_2O)_6$ complex: $\measuredangle(x, O_{12}\text{–}Al\text{–}O_{12}) = 27^\circ$, $\measuredangle(y, O_{13}\text{–}Al\text{–}O_{13}) = 27^\circ$, $\measuredangle(z, O_{11}\text{–}Al\text{–}O_{11}) = 19^\circ$. Apart from the experimental errors, one has to consider these deviations as regards the following aspects. The Al–O distances correspond rather exactly to the sum of the ionic radii of aluminium and oxygen. At a substitutional site these distances must become bigger because the ionic radius $R_{Cr} = 0.615$ Å of Cr^{3+} is larger than that of Al^{3+} by 0.045 Å. This expansion of the chromium-substituted $Cr_{Al}(H_2O)_6$ octahedron can result in a structural relaxation or rearrangement with respect to the neighbouring dimethylammonium and sulphate sites. The sensitivity of EPR to nearest-neighbour crystalline-field contributions is superior to that of NMR. Whereas the nuclear quadrupole tensor is determined by atomic monopole and dipole lattice sums converging slowly and making it dependent on distant atoms too [20], the EPR fine-structure tensor is mainly determined by the immediate environment of the paramagnetic ion. The temperature dependence of the EPR spectra in the X band and Q band were measured in selected directions from room temperature down to liquid helium temperature. Contrary to the ^{27}Al NMR results, not only were distinct line shifts observed with changing temperature but also a very strong line broadening already takes place in the ferroelastic phase where the linewidth grows from less than 5 mT at room temperature up to 50 mT at about 180 K. Surprisingly, below this temperature a line tripling of the fine-structure-split lines occurs for some directions already, far above the ferroelectric transition

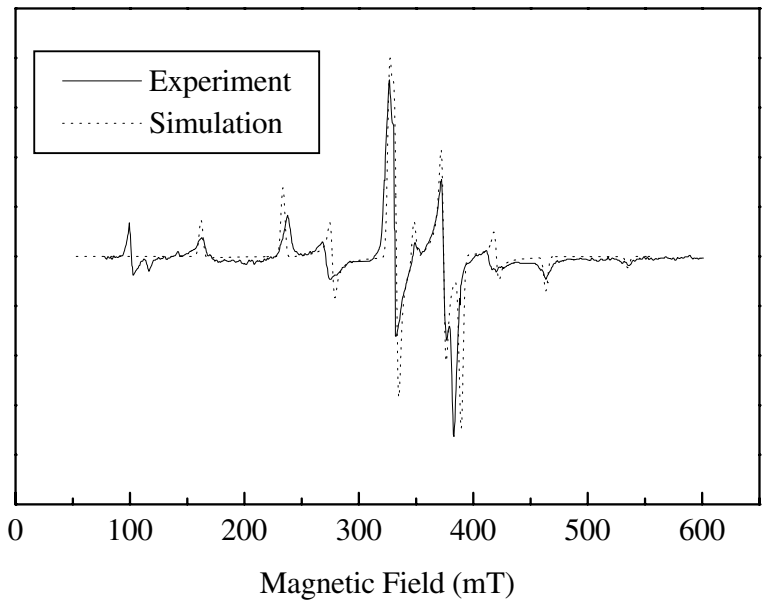

Figure 4. Experimental and simulated room temperature EPR powder spectra of Cr^{3+} in DMAAS measured at the X band. The simulation was done with the parameters given in the text. The forbidden lines appearing at about 100 mT were not included in the simulation as no forbidden transitions have been calculated.

temperature. The satellites of these triplets disappear in the ferroelectric phase and the lines narrow drastically on going to lower temperatures. Also a ferroelastic domain formation was observed after several cooling runs, manifested by new lines in the EPR spectra which follow the expected angular transformation. The effects mentioned become most clear in the Q-band EPR spectra. In particular, they were clearly observed in temperature-dependent EPR measurements with the magnetic field in the $\boldsymbol{a}^*\boldsymbol{c}$-plane at an angle of 20° with the $\boldsymbol{c}$-axis where the triplet lines show maximum fine-structure splitting and do not overlap with the other triplet.

Figure 5 shows a heating run for the magnetic field in the same plane but parallel to the $\boldsymbol{c}$-direction where the spectra of the two Cr^{3+} sites do collapse for symmetry reasons. Figure 5(a)

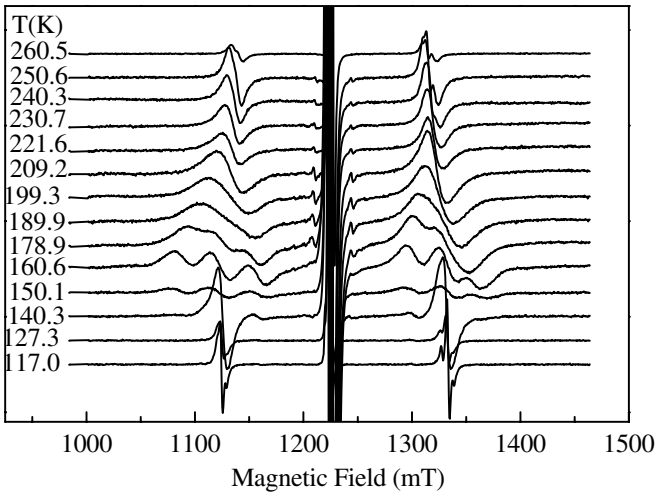

(a)

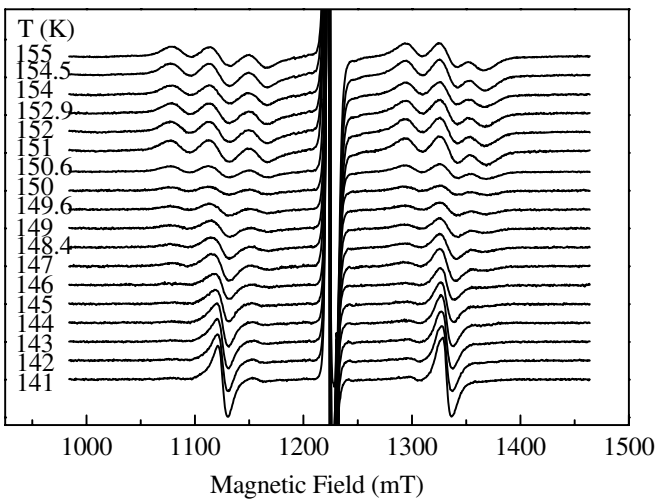

(b)

Figure 5. The temperature dependence of the Cr^{3+} EPR spectrum of DMAAS measured at the Q band with the magnetic field $\boldsymbol{B}$ parallel to the $\boldsymbol{c}$-direction (a) over a wide temperature range [17] (the splittings at the highest temperatures are due to slight misorientation) and (b) in the neighbourhood of the ferroelectric phase transition.

gives a survey of the dramatic spectrum changes occurring between 117 K and 260 K. The small splittings seen at low and high temperatures are due to a small sample misorientation. Figure 5(b) gives more detailed information on the spectrum changes in the near surroundings of the phase transition. The data analysis presented in the next section was carried out for this direction because here the most precise temperature measurements were performed.

4. Discussion

The Cr^{3+} ions are substituting for the isovalent Al sites in the centre of the water octahedron. The local site symmetry should remain inversionally symmetric as no charge compensation is necessary and also the ionic radii of the two ions are nearly equal. From this local inversion symmetry of the Cr^{3+} site it follows that there will be no line splittings that are linear in the ferroelectric order parameter, but only line shifts $\delta\nu$ proportional to the square of the order parameter η:

$$\delta\nu \sim \eta^2 \tag{2}$$

as is indeed observed in the ^{27}Al NMR experiments. One finds a simple explanation of the observed line tripling with intensity ratios 1:2:1 above the phase transition and the intensity transfer from the satellites to the central line of this triplet after passing the transition to the ferroelectric phase if one considers the influence of the order–disorder behaviour of neighbouring dimethylammonium molecules on the water octahedron. When the dimethylammonium molecule rotates around its C–C direction, the methyl protons approach closer than 1 Å to the water protons and may cause a distortion of the local crystalline field at the chromium site. This means that the Cr^{3+} fine-structure splitting is sensitive to the dimethylammonium arrangement. The structural situation around a chromium site is shown schematically in figure 6. Because we are interested in the behaviour at temperatures close to

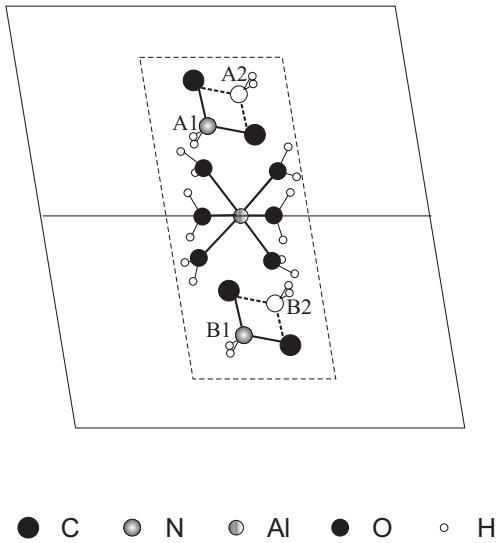

Figure 6. A schematic representation of the dimethylammonium-ion arrangements around an aluminium or chromium water octahedron projected on the $\boldsymbol{a}^*\boldsymbol{b}$-plane. Each of the two neighbouring dimethylammonium cations A and B can occupy one of the two polar positions 1 and 2. The shaded nitrogen positions correspond to the polar configuration A1–B1.

the transition temperature T_C, we may confine the considerations to the polar configurations of the two neighbouring dimethylammonium molecules called A1, A2 and B1, B2. Slightly above the phase transition, the chromium probes substituting at an aluminium site in a water octahedron find four possible configurations of the two neighbouring dimethylammonium groups: the configurations A1–B1 and A2–B2 which are inversionally symmetric with respect to one another and, therefore, give identical EPR lines forming the central line of the triplet, and the configurations A1–B2 and A2–B1, leading to the satellites at lower and higher field strength, respectively. The intensities of the triplet lines are a measure of the occupation probability of the four configurations. In the paraelectric phase where no preferential orientation of the dimethylammonium molecules exists, one expects an intensity ratio 1:2:1 in agreement with the experimental result. In the ferroelectrically ordered phase, the occupation probability depends on the order parameter η of the dimethylammonium reorientation:

$$\eta = (w_1 - w_2)/(w_1 + w_2) \tag{3}$$

where w_1 and w_2 mark the occupation probability for a dimethylammonium molecule in the polar position 1 or 2, respectively. The ratio r of the satellite line intensity I_S to the central-line intensity I_C is then given by

$$r = I_S/I_C = (1/2)(1 - \eta^2)/(1 + \eta^2) \tag{4}$$

which allows one to determine the local order parameter of the order–disorder behaviour of the dimethylammonium molecules.

In order to obtain correct intensity ratios from the experimental spectra, a deconvolution procedure was used which allows one to separate out the intensity contributions of each of the lines of the experimental line triplet by consideration of its line shape. Figure 7 shows the temperature dependence of the ratio $r = I_S/I_C$ calculated from the EPR spectra presented in figure 5. The transition temperature is determined to be $T_C = 151.1$ K. The order parameter of the dimethylammonium reorientation calculated from these data according to equation (4) is designated as η_{EPR1}. Its temperature dependence, already shown in our previous paper [17], is presented in figure 8 (full circles).

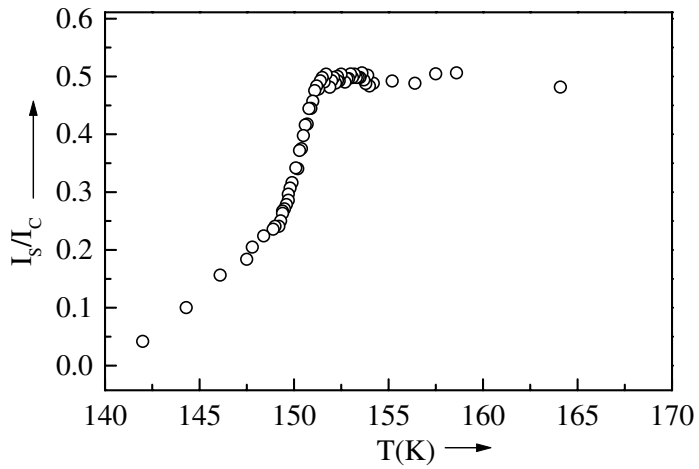

Figure 7. The temperature dependence of the intensity ratio I_S/I_C of the satellite and central-line intensities in the triply split EPR fine-structure line at lower field.

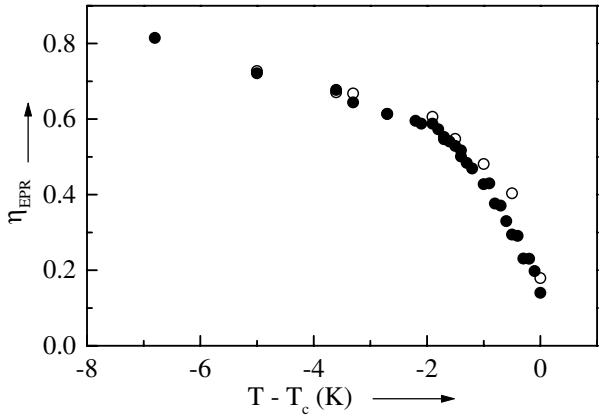

Figure 8. The temperature dependence of the local order parameters η_{EPR1} (full circles) and η_{EPR2} (empty circles) of the dimethylammonium reorientation determined from the triplet intensity ratio of the fine-structure-split Cr^{3+} lines according to equation (4) and from the temperature shift of the central-triplet-line frequency below T_C using equation (2), respectively.

Taking it into consideration that the measured line shift of the central triplet line must be proportional to the square of the order parameter (equation (2)), there is a second possibility for determining the local order parameter. It is called η_{EPR2} and shown as open circles in figure 8.

It is interesting to note that the ^{27}Al NMR results [15] give a similar temperature dependence of the order parameter designated as η_{NMR}. The temperature dependences of the local order parameters η_{EPR1}, η_{EPR2} and η_{NMR} obtained by EPR and NMR measurements are shown in figure 9 as full and open circles and open squares. In this figure, these local order parameters are compared with the results of spontaneous polarization measurements presented in reference [22]. The temperature dependence of the spontaneous polarization P_S has been

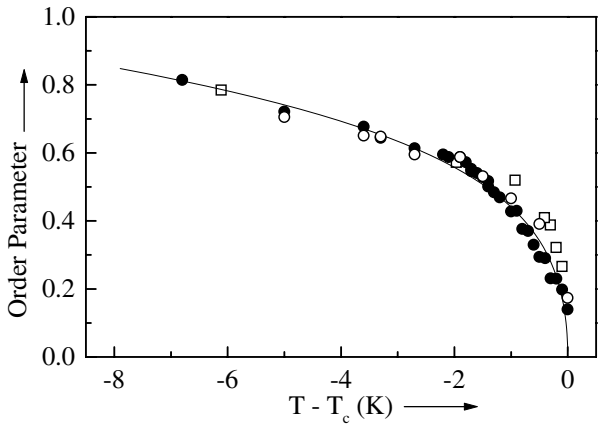

Figure 9. The temperature dependence of the local order parameters η_{EPR1} and η_{EPR2} (full and empty circles) of the dimethylammonium reorientation determined by means of EPR, of the local order parameter η_{NMR} (open squares) determined by means of NMR and of the electric spontaneous polarization P_S (solid line) plotted on a normalized order parameter scale. The magnitudes of η_{EPR2}, η_{NMR} and P_S are adapted to that of η_{EPR1} at $T_C - T = 4$ K. The experimental P_S-values are represented by the state equation, equation (5), with the parameters given in the text.

shown to follow the state equation

$$T_C - T = \beta P_S^2 + \gamma P_S^4 \tag{5}$$

for $T_C - T \leqslant 4$ K where $\beta = B/A_0$ and $\gamma = C/A_0$ with $A_0 = 3.7 \times 10^7$ V m C^{-1} K^{-1}, $B = 3.5 \times 10^{11}$ V m^5 C^{-3} and $C = 4.2 \times 10^{15}$ V m^9 C^{-5}. A_0, B and C are the coefficients of the Landau expansion of the free enthalpy:

$$G = \frac{A_0}{2}(T - T_C)P_S^2 + \frac{B}{4}P_S^4 + \frac{C}{6}P_S^6. \tag{6}$$

The line drawn in figure 9 was calculated according to equation (5) with the given parameters. As the order parameter values determined by means of the different techniques are proportional to one another but not equal in magnitude, they were adapted to the normalized order parameter values obtained from the triplet intensity ratio at $T_C - T = 4$ K. The present results evidently confirm the order–disorder character of the ferroelectric transition in DMAAS on a microscopic level and give additional indication for a nearly tricritical behaviour.

In addition to the above-discussed intensity behaviour of the line triplet, there are very striking line broadenings and also variations of the line separation (see figures 5(a) and 5(b)) indicating changes in the dynamics of the dimethylammonium motion. Assuming an independent reorientation of the dimethylammonium molecules, the motional model of the chemical exchange between four sites [21] may be used for determining the reorientational correlation time τ. The resonance frequencies ω_n of these sites corresponding to the four dimethylammonium configurations discussed above are marked as $\omega_2 = \omega_3 = \omega_0$, $\omega_1 = \omega_0 - \Delta_0$, $\omega_4 = \omega_0 + \Delta_0$ when no exchange takes place. In the exchange process, the site n is occupied with the probability P_n. The shape of the EPR absorption line is then given by

$$I(\omega) = \mathrm{Im}\left[\left(\mathrm{i}\omega_r M_0 \sum_{n=1}^{4} P_n/(1+\alpha_n\tau)\right)\Big/\left(\sum_{n=1}^{4} P_n\alpha_n/(1+\alpha_n\tau)\right)\right] \tag{7}$$

with

$$\alpha_n = \Gamma_0 + \mathrm{i}(\omega_n - \omega) \tag{8}$$

where Γ_0 is the basic linewidth and ω_r is the amplitude of the microwave field B_1 in frequency units. For fast reorientations the triplet is reduced to only one line and the correlation time τ can be taken from the measured linewidth Γ whereas in the region of transition to the slow-motion regime the correlation time of the reorientation can be calculated from the reduced triplet splitting Δ. For both cases, the correlation time of the reorientation was ascertained by numerical calculations of linewidth and line splitting using equation (7). Line-shape simulations showed that a temperature-dependent basic linewidth

$$\Gamma_0 = \frac{1}{1.8\Delta_0 + 1/(5\tau)} \tag{9}$$

has to be used where the temperature dependence has been introduced via τ. The changes of line shape and linewidth with temperature shown in figure 5(a) have been simulated successfully by means of equation (7) as demonstrated in figure 10.

From the dynamic behaviour of the dimethylammonium molecules it becomes evident that the difference in temperature behaviour of the NMR and EPR spectra is related to the difference in timescale of the two experiments with respect to the dimethylammonium reorientational motion. On the timescale of the NMR measurements given by the relevant quadrupolar splittings of less than 1 MHz [15], the dimethylammonium reorientational motion with a frequency larger than 100 MHz appears to be always fast. Consequently, the NMR line shifts due to the different local dimethylammonium arrangements around the Al sites

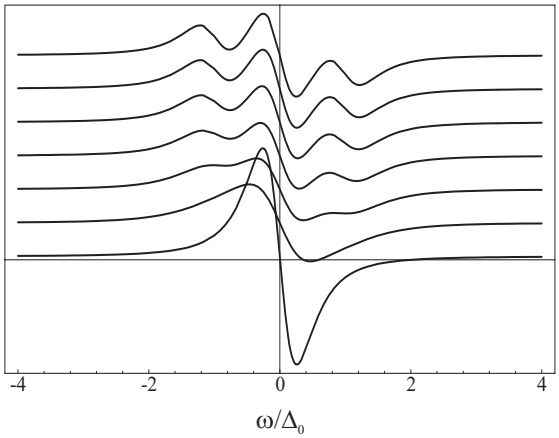

Figure 10. Simulation of the triply split EPR fine-structure line shown on a normalized frequency scale ω/Δ_0 using equations (7), (8) and (9) for normalized reorientation times $\tau\Delta_0 = 0.1$ (bottom) to 6.1 (top) in steps of 1.0.

are averaged out and only one single line appears at all temperatures. The timescale of the EPR experiment, however, is given by the triplet splitting of about 35 mT corresponding to about 1000 MHz. Consequently, above the phase transition the dimethylammonium motion is already slow enough to make the different arrangements distinguishable in the EPR spectrum.

The analysis of the experimental spectra results in a temperature dependence of the correlation time τ of reorientation as for an order–disorder transition driven by a relaxational mode [23]. As shown in figure 11, the correlation time τ above T_C can be represented by

$$1/\tau = a|T - T_C| \exp(-E/kT) + b \tag{10}$$

with an estimated activation energy $E/k = 790$ K and parameters $a = 3.5 \times 10^{10}$ K^{-1} s^{-1} and $b = 7 \times 10^8$ s^{-1}. The here-determined relaxation times of the dimethylammonium reorientational motion are shorter by two orders of magnitude than the relaxation times determined by dielectric measurements [24]. The reason for this difference is presumably that in the present ESR experiment the average reorientation time of the individual dimethylammonium molecules is measured but not the relaxation time of the electric polarization fluctuations as in the case of dielectric measurements. In other words, the EPR experiment does not reflect just the dynamics at the critical wave vector as does dielectric relaxation but sums over the whole wave-vector space.

At the phase transition temperature the dimethylammonium reorientation time stays finite with a value of about 10^{-9} s. Inside the ferroelectric phase it is decreasing again with lower temperatures. As in the case of hydrogen-bonded ferroelectrics in the ferroelectric phase, the residence time τ^+ of the dimethylammonium molecules in the rotational potential minimum of the preferential direction is longer than τ^- in the opposite minimum leading to a finite net polarization. The same behaviour is true also above T_C. Fluctuations of the two 'polar' rotational potential minima lead to polarization fluctuations with a lifetime that is much longer then the rotation rate of the DMA molecules. This behaviour could also be reinforced by a coupling of the dimethylammonium order to other polar molecular units in the lattice such as the sulphate molecules and the hydrogen bonds.

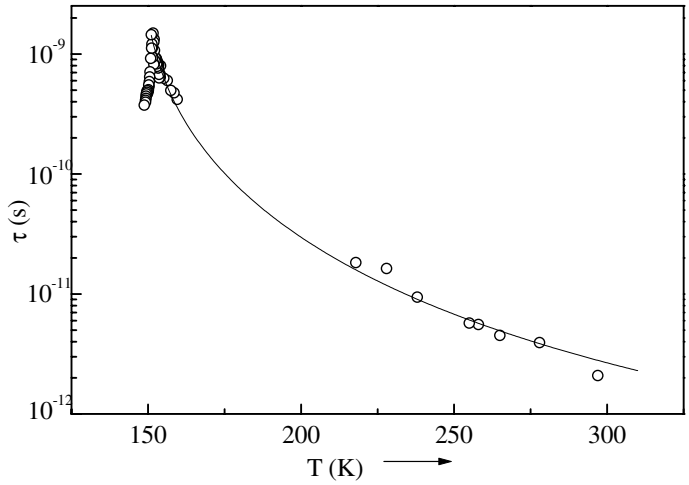

Figure 11. The temperature dependence of the correlation time τ of the dimethylammonium reorientation determined from the triplet splitting and linewidth of the fine-structure-split Cr^{3+} EPR line using equations (7), (8) and (9). Two experimental measurements with $\boldsymbol{B}$ in the $\boldsymbol{ac}$-plane were evaluated. The line shows the fit result for $T > T_C$ obtained using equation (10) with the parameters given in the text.

5. Conclusions

We have demonstrated that electron paramagnetic resonance (EPR) provides a very direct opportunity to study the reorientational order and dynamics of the polar dimethylammonium units in DMAAS via their influence on the crystalline field of the paramagnetic Cr^{3+} probe substituting at the aluminium sites. The reason for the difference in temperature behaviour of the ^{27}Al NMR and Cr^{3+}_{Al} EPR lines is the difference in timescale of the experiments with respect to the dimethylammonium rotational frequency. The latter is always extremely large with respect to the relevant frequencies of the NMR quadrupolar splittings ($\sim$1 MHz) but is of similar magnitude to those of the EPR splittings ($\sim$1 GHz). This explains why remarkable line-shape changes and line splittings are observable only in the EPR experiment. The EPR measurements in chromium-doped DMAAS single crystals confirm the order–disorder character of the ferroelectric phase transition at 151 K on a microscopic level and give information about the critical behaviour of the order parameter. The local order parameter of the DMA reorientation shows the same temperature dependence as the spontaneous polarization. The critical fluctuations measured in the dielectric relaxation are related to fluctuations of the rotational potential minima of the DMA groups. The dynamics of the individual DMA rotational reorientation never freezes out, however, and is always faster than the extremely slow critical relaxation of the electric polarization fluctuations.

Acknowledgments

The authors are very grateful to Professor J Grigas for stimulating discussions. Some of the authors acknowledge the support by the Volkswagen-Stiftung (NA, DM, ZC, JF) and by the Deutsche Forschungsgemeinschaft (GV).

References

[1] Kirpichnikova L F, Shuvalov L A, Ivanov N R, Prasolov B N and Andreyev E F 1989 *Ferroelectrics* **96** 313
[2] Vlokh O G, Kapustianik V B, Polovinko I I and Sveleba S A 1990 *Ferroelectrics* **111** 333
[3] Kirpichnikova L F, Urusovskaya A A, Shuvalov L A and Mozgovoy V I 1990 *Ferroelectrics* **111** 339
[4] Kirpichnikova L F, Ivanov N R, Gavrilova N D, Dolbinia V V, Slabkova G L and Shuvalov L A 1991 *Sov. Phys.–Crystallogr.* **36** 702
[5] Kirpichnikova L F, Urusovskaya A A, Mozgovoi V I, Kiosse G A and Razdobreev I M 1991 *Sov. Phys.–Crystallogr.* **36** 859
[6] Kapustianik V, Bublyk M, Polovinko I, Sveleba S, Trybula Z and Andreyev E 1994 *Phase Transitions* **49** 231
[7] Kiosse G A, Razdobreev I M, Kirpichnikova L F, Malinovskii T L and Shuvalov L A 1994 *Crystallogr. Rep.* **39** 27
[8] Kapustianik V, Polovinko I and Kaluza S 1996 *Phys. Status Solidi* a **153** 117
[9] Dacko S and Czapla Z 1996 *Ferroelectrics* **189** 143
[10] Pietraszko A, Lukaszewicz K and Kirpichnikova L F 1993 *Pol. J. Chem.* **67** 1877
[11] Kapustianik V, Fally M, Kabelka H and Warhanek H 1997 *J. Phys.: Condens. Matter* **9** 723
[12] Pietraszko A and Lukaszewicz K 1994 *Pol. J. Chem.* **68** 1239
[13] Kazimirov V Yu, Rieder E E, Sarin V A, Shuvalov L A and Fykin L E 1998 *Kristallografiya* **43** 228
[14] Kazimirov V Yu, Sarin V A, Ritter C and Shuvalov L A 1999 *Kristallografiya* **44** 61
[15] Alsabbagh N, Michel D, Furtak J and Czapla Z 1998 *Phys. Status Solidi* a **167** 77
[16] Dolinšek J, Klanjšek M, Arčon D, Kim Hae Jin, Seliger J and Žagar V 1999 *Phys. Rev.* B **59** 3460
[17] Völkel G, Alsabbagh N, Böttcher R, Michel D and Czapla Z 1999 *Phys. Status Solidi* b **215** R5
[18] Bednarski W, Waplak S and Kirpichnikova L F 1999 *J. Phys.: Condens. Matter* **11** 1567
[19] Abragam A and Bleaney B 1970 *Electron Paramagnetic Resonance of Transition Ions* (Oxford: Clarendon)
[20] Müller K A and Fayet J C 1991 *Structural Phase Transitions* II ed K A Müller and H Thomas (Berlin: Springer) pp 1–82
[21] Johnson C S 1965 *Advances in Magnetic Resonance* vol 1, ed J S Waugh (New York: Academic) pp 33–102
[22] Cach R, Dacko S and Czapla Z 1989 *Phys. Status Solidi* a **116** 827
[23] Blinc R and Žekš B 1974 *Soft Modes in Ferroelectrics and Antiferrelectrics* (Amsterdam: North-Holland)
[24] Sobiestianskas R, Grigas J, Samulions V and Andreyev E F 1991 *Phase Transition* **29** 167
[25] Czapla Z and Tchukvinskyi R 1998 *Acta Phys. Pol.* A **93** 528
[26] Sobiestianskas R, Grigas J, Andreyev E F and Varikash V M 1992 *Phase Transition* **40** 85